International Journal of Science and Research (IJSR)
ISSN: 2319-7064
Index Copernicus Value (2016): 79.57 | Impact Factor (2017): 7.296

Investigation of Broken Rotor Bar Fault in Field Oriented Controlled Induction Motor Using Discrete Wavelent Transform

Iwunze Nnadozie[1], Izuegbunam Fabian I[2], AkwukwaegbuIsdore O[3]

Electrical and Electronic Engineering, Federal University of Technology, Owerri, Nigeria

Abstract: ***Fault diagnosis of Induction motor has been successfully done using motor current signature analysis. However, this technique is not effective with non-stationary signal associated with varying-load operation. With current development in motor drives, precise control techniques like field oriented control tend to mask the effect of fault, making diagnosis more difficult. This has prompted the application of Wavelet transform, a multi-resolution signal processing technique that can capture transient features.This paper investigates the effect of Broken Rotor Bar (BRB) fault in motor stator current using discrete wavelet transform to validate the robustness of wavelet diagnostic procedure over control regulator parameters and motor load. To achieve this, BRB fault is modelled in MATLAB/Simulink and the sampled signal processed using MATLAB commands. The results show that detail coefficient plot that correspond to low frequency range between 39Hz and 156Hz provide relevant information about fault presence where the operating frequency is 50Hz. The amplitude variation with severe conditions further makes discrete wavelet transform an effective fault scaling tool for field oriented controlled induction motor.***

Keywords: Induction motor, Broken rotor bar, Motor current signature analysis, Field oriented control, Fast Fourier transform, Discrete wavelet transform.

1. Introduction

Over the years, induction machines have provided the most common form of electromechanical power for industrial, commercial and domestic applications at constant speed; this is because of its comparativecost advantage, simplicity, stability ruggedness, ease in maintenance.Despite these advantages, they are still subjected to different faults due to wear and tear, transient conditions, rotating nature of machines, operating environment and aging. In addition to these faults is the effect of electrical asymmetry due to broken bars in squirrel cage induction motor. This develops as crack at the junction of end-rings of the rotor causing healthy bars to conduct more current that increase the possibility of further cracking due to stress.

Sudden breakdownassociated with these faults could lead tohuge financial losses, down-time, and accident at workplace. While a nascent BRB fault may not cause immediate failure especially in multi-pole (slow-speed) motor, it can lead to deterioration of other components consequently, increasing both time and cost of maintenance. To this end, studies have been carried-out to develop monitoring and fault detection system that will detect these faults at its incipient or localized stage where its maintenance can involve only a fraction of the cost of motor replacement.

Motor Current Signature Analysis (MCSA) has been widely studied in detecting different faults in induction motor [1-3].A vital point about this technique is that it analyses electrical signal that contains frequency components that are a direct by-product of unique rotating flux components caused by faults such as broken rotor bars, air-gap eccentricity, and shorted turns. This is the basis for the wide application of MCSA in detecting faults. In all cases,Side-bands extracted from spectrum analysis of stator current signal are the dominant fault indicator. The study [4], observed that the side-bands are influenced by load-levels, such that itsresult is reliable only at rated load operation of induction motor, which becomes a limitation where varying load operation is desired.

However, the introduction of Adjustable Speed Drives (ASDs) has improved the motor efficiency, control, energy management and widened its applications. Studies by [5-6],showed that certain variables employed for diagnosis in open loop were no longer effective in closed-loop where drive was in use.Also [7] remarked that inverter supply brings a slight advantage of additional components in low frequency spectrum and increased amplitude of even harmonics which can enhance detection, motor behaviour. This implies that the control action may scramble the effects of known fault signatures such voiding precision associated with the usual index. With the development in powerelectronics and digitalprocessing control strategies has improved, a widely used control scheme today is the Field Oriented Control scheme (FOC) which imitates DC motor operation using mathematical transformations to decouple torque and flux, such that both quantities can be controlled independently to obtain desired motor speed and operation. In [8] a comparison of different fault alert signals was investigated for FOC motors and the experimental result showed that the analysis of motor input current is simple and effective.Faulty motors withdifferent control strategies when compared, indicatedthat the type of control strategy in use affects reliability of diagnosis [9].

The classic frequency analysis based signal processing technique of current signal using the application of frequency based signal processing techniques like Fast Fourier Transform (FFT) or Short-Time Fast Fourier Transform (STFFT) has proved inefficient for non-sinusoidal signal which properly describes current signals in

FOC application. Wavelet transform is drawing increasing attention in fault diagnosis because of its advantage of providing time-frequency information with good resolution.It has been deployed in online and offline diagnosis of wound rotor machine, applied for varying load operation, used for analysis of start-up current signal [10-12]. In all cases, it successfully detected fault. Fault quantification has also been considered with Discrete Wavelet Transform(DWT). The use of DWT indexes like Root Mean Square of the wavelet coefficient to estimate the extent of fault recorded reasonable success that opened door to application of artificial intelligenceprogram [13].

In this paper, the method for diagnosing broken rotor bar fault using discrete wavelet transform of current signal is described in a MATLAB/Simulink work environment. The coefficient plots that referred to the scale-time representation of the signal is observed for both healthy and faulty conditions.

2. Methodology

In developing a reliable fault detection scheme to detect broken rotor bar fault, a three-phase induction motor operating with a broken rotor bar fault has to be studied and compared with a healthy motor. To achieve this, a healthy three phase motor is modelled using Simulink,while broken rotor bar fault effect is introduced as variation in resistance of the motor. The stator current signal is extracted from the simulation output and fed into a discrete wavelet transform signal processing block. The waveforms for healthy motor and faulty motor is compared to identify fault signals.

Wavelet Transform

Wavelet transform is a tool that decomposes a time domain signal into different scales (various levels of smaller frequency spectra) with different levels of resolution by dilating a single prototype function referred to as mother wavelet. Using variable-sized regions that allow the use of long time intervals for a more precise low-frequency information and shorter regions for high frequency information.

DWT splits a signal into several band-limited signals, the sum of which produces the original signal. It employs two sets of functions; the scaling function and the wavelet function to yield detail and approximate information of the signal [14]. DWTcan be considered as passing a signal through digital filter banks, the original signal x[n] is passed through low-pass filter G[n] and high-pass filter H[n] which produces detail and approximate coefficients respectively; the output of the low-pass filter is further decomposed in the subsequent filter bank. This continues till two sample are left within close frequency range. A multilevel decomposition of a signal using DWT is shown in fig.3

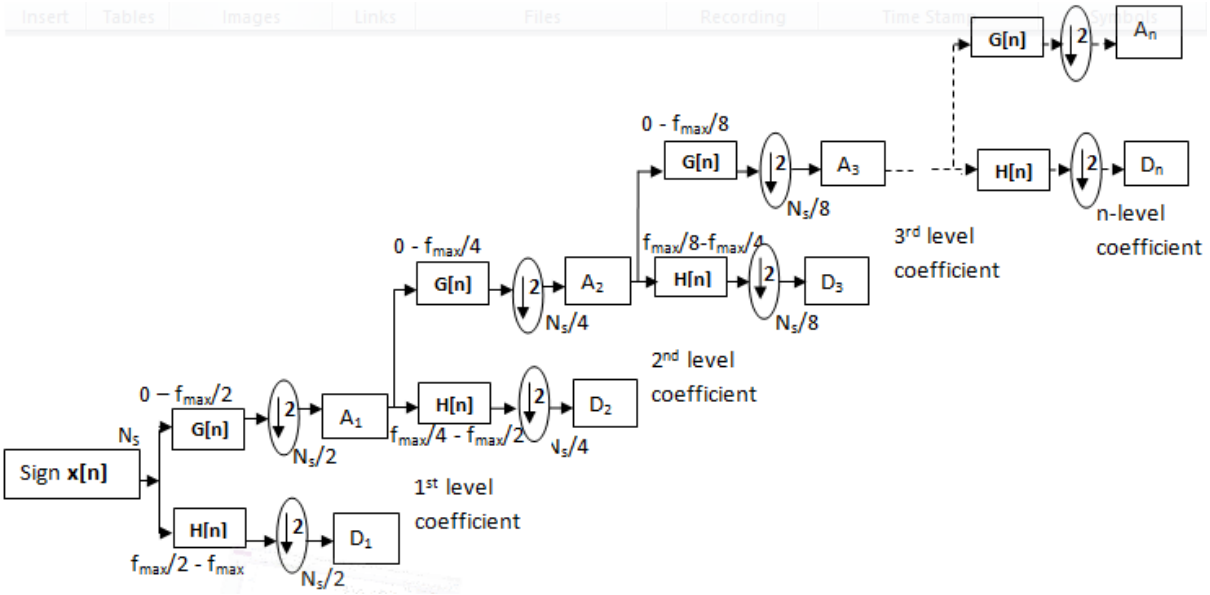

Figure 3: Multi-level Wavelet Decomposition

For each filter operation, the frequency of the signal is halved while the sample width remains the same. Applying Nyquist rule, half of the samples can be discarded, such, the operator↓2 denotes the down-sampling of the signal by an integer 2. The down sampling causes high frequency signal components to be misinterpreted by subsequent filter banks, a form of distortion referred to as aliasing.

This aliasing effects is cancelled out using appropriate reconstruction filters by a process referred to as synthesis. This is done by reconstructing the original detail and approximations from the coefficients by up sampling and using filters as shown in fig. 4.

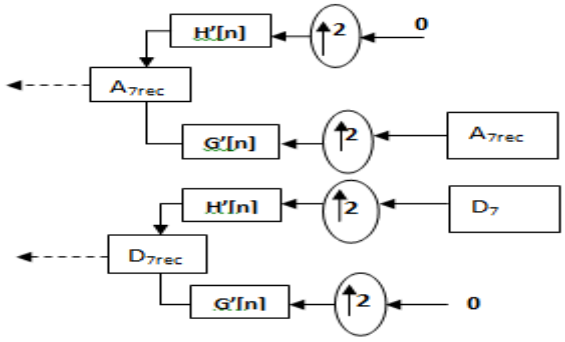

Figure 4: Detail and Approximation Coefficient Reconstruction

The coefficient vector A is passed via the reconstruction filters G'[n] and H'[n], but this time, a vector of zero is feed in place of the detail coefficient. This applies to the reconstruction of detail coefficient as well.

The major advantage of wavelet transform is the availability of abundant mother-wavelets that offer a range of abilities that include orthogonality, symmetry and compact support. Daubechies mother-wavelet has been employed in this paper to avoid low level overlapping with adjacent bands. The properties of this family can be obtained using "*waveinfo*('db')" command in MATLAB.

Motor Model

The model of the induction motor is derived by using d and q variables in a synchronously rotating reference frame. The Simulink model for 3-phase squirrel-cage implemented in this paper is shown in Fig.5, whichconsists of the transformation blocks and motor dq-model.

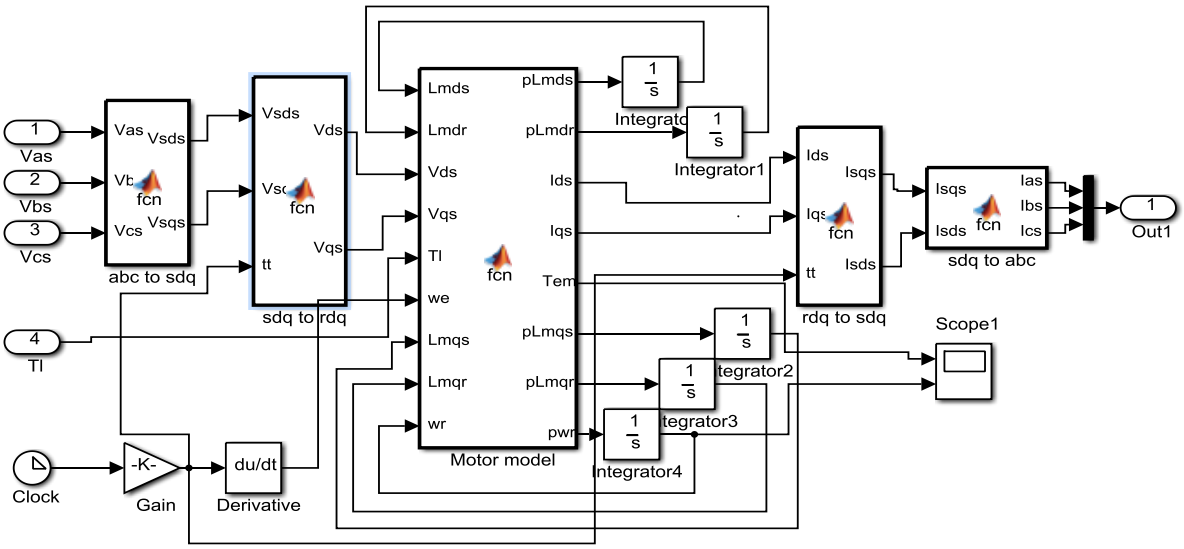

Figure 5: Simulink Model of Induction Motor

Three-phase(abc) variables (voltage, current or flux-linkage) are converted to 2-phase synchronously rotating frame(d-q), by first converting to the 2-phase stationary frame(α, β) and then from (α, β) to the desired synchronous rotating frame (d,q) using the transformation matrix in equation (2) and (3). The dq-abc transformation does the opposite of the abc-dq conversion.

$$\begin{bmatrix} f_\alpha \\ f_\beta \end{bmatrix} = 2/3 \begin{bmatrix} 1 & -1/2 & -1/2 \\ 0 & \sqrt{3}/2 & -\sqrt{3}/2 \end{bmatrix} \cdot \begin{bmatrix} f_a \\ f_b \\ f_c \end{bmatrix} \quad (2)$$

$$\begin{bmatrix} f_d \\ f_q \end{bmatrix} = \begin{bmatrix} \cos\theta & \sin\theta \\ -\sin\theta & \cos\theta \end{bmatrix} \cdot \begin{bmatrix} f_\alpha \\ f_\beta \end{bmatrix} \quad (3)$$

The d-q model of the induction motor is derived based on the mathematical model described by the following equations [15].

Voltage equation

$$\left.\begin{aligned} V_{qs} &= r_s i_{qs} + p\lambda_{qs} + \omega\lambda_{ds} \\ V_{ds} &= r_s i_{ds} + p\lambda_{ds} - \omega\lambda_{qs} \\ V_{qr} &= r_r i_{qr} + p\lambda_{qr} + (\omega - \omega_r)\lambda_{dr} \\ V_{qr} &= r_r i_{dr} + p\lambda_{dr} - (\omega - \omega_r)\lambda_{qr} \end{aligned}\right\} \quad (4)$$

Flux Linkages in matrix form

$$\begin{bmatrix} \lambda_{ds} \\ \lambda_{qs} \\ \lambda_{dr} \\ \lambda_{qr} \end{bmatrix} = \begin{bmatrix} L_{ls}+l_m & 0 & L_m & 0 \\ 0 & L_{ls}+L_m & 0 & L_m \\ L_m & 0 & L_{lr}+L_m & 0 \\ 0 & L_{lr}+L_m & 0 & L_m \end{bmatrix} \cdot \begin{bmatrix} i_{ds} \\ i_{qs} \\ i_{rd} \\ i_{rq} \end{bmatrix} \quad (5)$$

Torque equation

$$\left.\begin{aligned} T_{em} &= \frac{3}{2}\frac{p}{2\omega_r}\left(\lambda_{qr} i_{dr} - \lambda_{dr} i_{qr}\right) \\ T_{em} &= \frac{3}{2}\frac{p}{2\omega_r}\left(\lambda_{ds} i_{qs} - \lambda_{qs} i_{ds}\right) \end{aligned}\right\} \quad (6)$$

Speed equation

$$\frac{J}{p} p\omega_r = (T_{em} - T_l) \quad (7)$$

Model of Broken Rotor Bar Fault

Broken Rotor bars and end rings are usually associated with thermal stresses, magnetic stresses due to electromagnetic forces, residual stresses due to manufacturing and environmental stresses that are caused by moisture, humidity or chemical [16]. Some of the causes of these stresses include;

- A direct-on-line starting duty cycle for which the rotor cage winding was not designed to withstand, causes high thermal and mechanical stresses.
- Pulsating mechanical loads such as reciprocating compressors or coal crushers and so on can subject the rotor cage to high mechanical stresses.
- Imperfections in the manufacturing process of the rotor cage.

Rotor faults start as cracks at the end rings or small holes through the conducting bar. Different motor parameters such as pulsations in the speed, air gap flux, vibrations and motor current signature can be monitored for the detection of BRB

faults. Early fault detection techniques for these motors can significantly reduce the maintenance costs.

The broken rotor model is based on the equivalent circuit of rotor cage electrical connections obtained with the following assumptions;

1) Magnetomotive forces are sinusoidal
2) Non-saturation of magnetic circuit and negligible skin effect

A crack or break in any of the bars causes asymmetry of the resistance and inductance in rotor phases, which result in asymmetry of the rotating electromagnetic field in the air–gap between stator and rotor. Consequently, this will induce frequency harmonics in the stator current. Rotor bar fault can therefore be modelled by unbalancing the rotor resistance and inductance.

In this paper, a model proposed and verified by Chen and Zivanovic[16]is adopted in modelling broken rotor bar fault. The model breaks down the effect of rotor break to a change in rotor resistance Rr, the inductance change is neglected due to its insignificance compared with change in resistance. For simplicity, the effect of the rotor end ring is neglected and it is assumed that the resistance and inductance of the stator did not change.

Per-phase rotor equivalent resistance for healthy motor is given by,

$$r_{rabc} = \frac{2(n_s)^2}{n_b/3} r_r \quad (8)$$

Where n_s and n_b are number of stator turns and number of rotor bars respectively;where n_{bb} is the number of broken bars, thenper-phase modified equivalent resistance for motor with BRB is expressed as,

$$r_{rabc}{}^* = \frac{2(n_s)^2}{\frac{n_b}{3} - 3n_{bb}} r_r \quad (9)$$

Per-phase increment in rotor resistance due to BRB fault is calculated as,

$$\Delta r_{rabc} = r_{rabc}{}^* - r_{rabc} = \frac{3n_{bb}}{n_b - 3n_{bb}} r_r \quad (10)$$

Field Oriented Control (FOC) Operation

The objective of FOC is to independently control torque and flux as it is in separately excited DC motor. This is done by choosing a d-q rotating reference frame synchronously with the rotor flux space vector. Once orientation is achieved, the torque and flux producing current can be decoupled and precise control can be achieved. A limiting feature of field orientation is the method whereby the rotor angle (Orientation) is acquired or estimated. Based on this, two types of FOC in use include the Direct FOC (DFOC) and Indirect rotor FOC (IR-FOC). In DFOC, the rotor angle is obtained directly using measurement instruments like the sensing coil mounted on the motor air-gap, while in Indirect rotor FOC, rotor angle is estimated using slip relation that require measurement of rotor speed.

Considering the d-q model of the induction machine in the reference frame rotatingat synchronous speed ω_e,the field-oriented control implies that the i_{ds}component of the stator current wouldbe aligned with the rotor field and the i_{qs}component would be perpendicular to i_{ds}. This can be accomplished by choosing $\omega_e$as speed of the rotor flux and locking thephase of the reference frame system in a manner that the rotor flux is aligned precisely with the d-axis, such that$\lambda_{qr} = 0,\ \lambda_{qr} = 0,\ \lambda_r = \pi_{qr}$

Using the flux linkage equations, torque equation can be written as,

$$T_{em} = \frac{3}{2}\frac{p}{2}\frac{L_m}{L_r}\pi_{dr} l_{qs} = 0 \quad (11)$$

This establishes the fact that torque can be controlled by varying the q-axis component of stator current

Similarly, the rotor flux equation $\lambda_{dr} = l_m i_{ds} + l_r i_{dr}$ can be reduced to

$$\lambda_r = l_m i_{ds} \quad (12)$$

From the voltage equations, slip speed is obtained as,

$$\omega_{sl} = \omega_s - \omega_r = \frac{r_r l_m l_{qs}}{L_r \pi_r} \quad (13)$$

For an IR-FOC, the rotor position is obtained with the equation,

$$\theta_e = \int (\omega_{sl} + \omega_r) dt \quad (14)$$

The implemented control architecture is shown in the fig.6

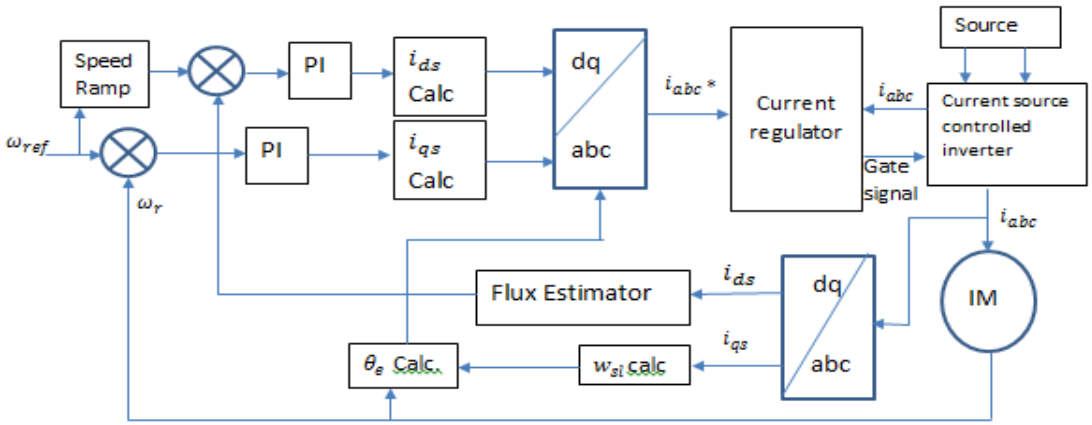

Figure 6: Field Oriented Control Architecture

It is observed that apart from the speed PI controller that generate the reference value of the torque-producing current componenti_{qs}, an additional controller is included in this architecture which is the flux PI that generates the reference

flux producing current component i_{ds}.This PI controller compares the estimated value (speed or rotor flux) and the reference value as the input to a Proportional Integrator which calculates the value of the variable to be applied to the motor.

Simulation of Broken Rotor Bar Fault

An induction motor driven with FOC motor drive is modelled in MATLAB/Simulink work environment as shown in fig.7.

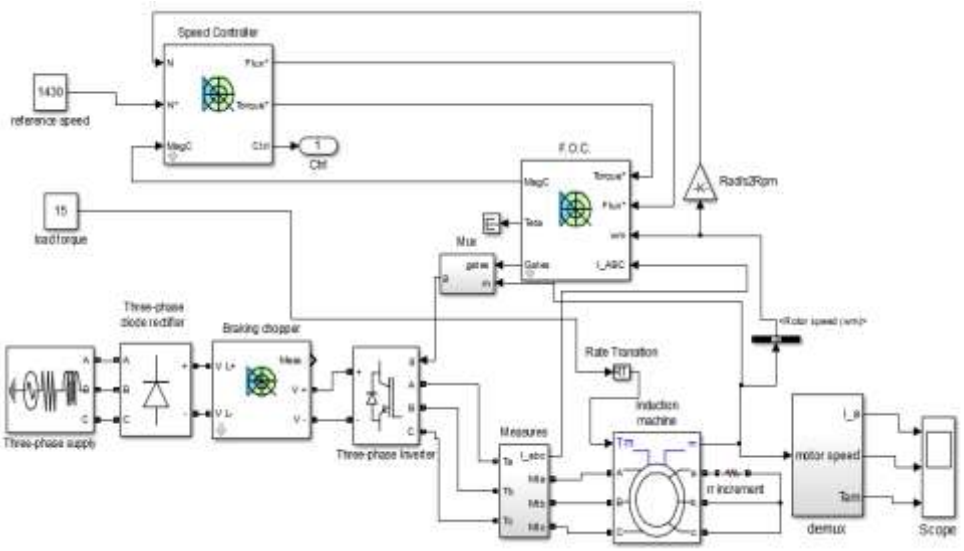

Figure 7: Simulink Model of FOC Motor with BRB Fault

BRB fault is realized by incremental resistance calculated using equation 13 such that break of one bar corresponds to Δr_r=0.0979. The parameters of induction motor used in the simulation are shown in table.1.

Table 1: Parameter of Induction Motor used

Parameters of the Induction Motor Used	
Rated power	3Hp/2238W
Rated phase voltage (Vrms)	220V
Rated frequency (f)	50Hz
No. of poles (P)	4
Stator winding resistance (Rs)	0.435Ω
Stator winding Inductance (Ls)	2e-3H
Rotor winding resistance (Rr)	0.816Ω
Rotor winding Inductance (Lr)	2e-3H
Mutual inductance (Lm)	69.13e-3H
Moment of Inertia (J)	0.089kg.m^2
Friction factor	0.005Nms
No. of rotor bars	28

Multi-level discrete wavelet decomposition of phase current sampled at 5000HZ frequency gives seven levels of decomposition corresponding to different frequency bands as shown in table.2. ApplyingNyquist rule, bandwidth of 2500Hz is captured in the division into scale maintaining half of the bandwidth after each scale. The wavelet decomposition is carried-out on the command window using "*wavedec"*command, the multi-level reconstructed coefficient plotted for analysis is obtained using the "*wrcoef"* command.

Table 2: Frequency bands for the seven levels of wavelet signals

Decomposition Level	Frequency bands (Hz)
Detail at level 1 (d1)	1250-2500
Detail at level 2 (d2)	625-1250
Detail at level 3 (d3)	312-625
Detail at level 4 (d4)	156-312
Detail at level 5 (d5)	78-156
Detail at level 6 (d6)	39-78
Detail at level 7 (d7)	19-39
Approx. at level 7 (a7)	0-19

3. Results and Discussion

Fig.8shows the current, speed and torque plot against time for the test motor at no-load for healthy and faulty condition. To detect the broken bars fault, the wavelet coefficients (A7, D7 - D1) of phase-a of the stator current of both the healthy and faulty motor is plotted and shown in fig.9.

Fig.10 shows the stator current, speed and torque plot against time for healthy and faulty motor. In fig.11, the wavelet analysis of the phase-a of stator current is presented for detail-4 to detail-7 coefficient plot at full load and rated speed of 1500RPM. The simulation for fig.11 is repeated at reduced speed and the wavelet analysis id shown if fig.12. to detect severe broken rotor bar fault, detail-5 to approximate coefficient plot for 1BRB and 2BRB is compared in fig.13.

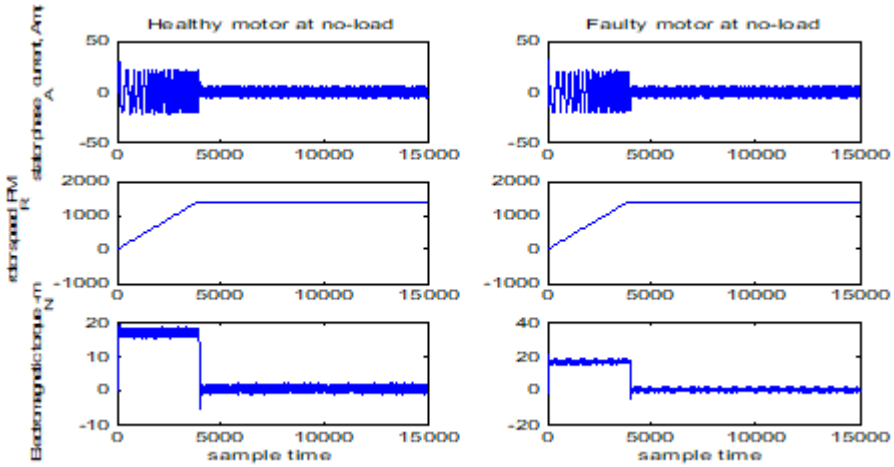

Figure 8: Current, Speed and Torque plot of motor at no-load

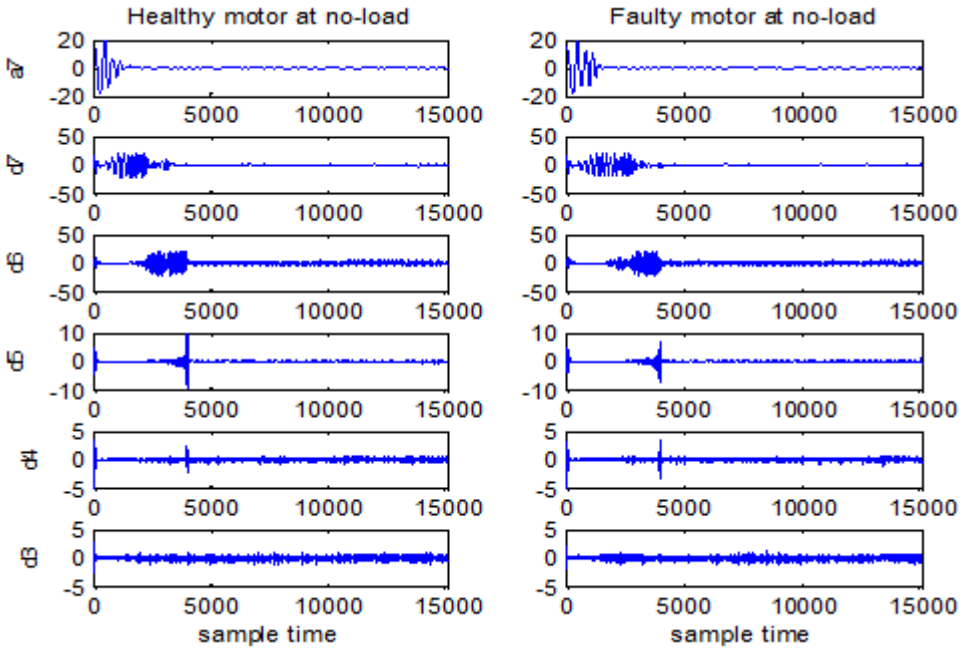

Figure 9: Wavelet coefficient plot of motor at no-load

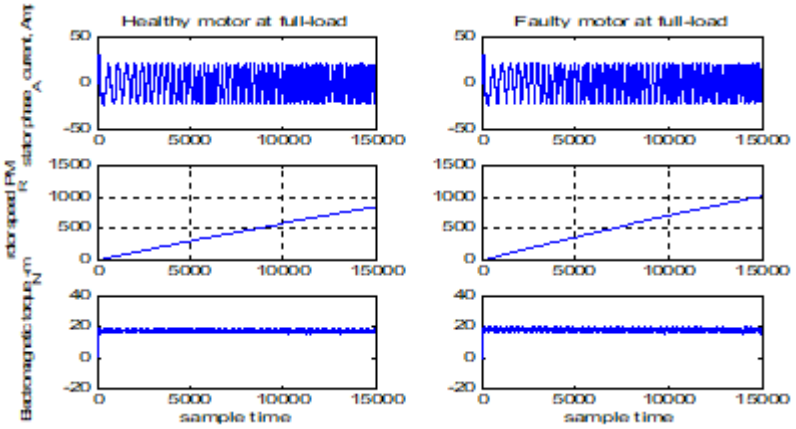

Figure 10: Current, Speed and Torque plots of motor at full-load

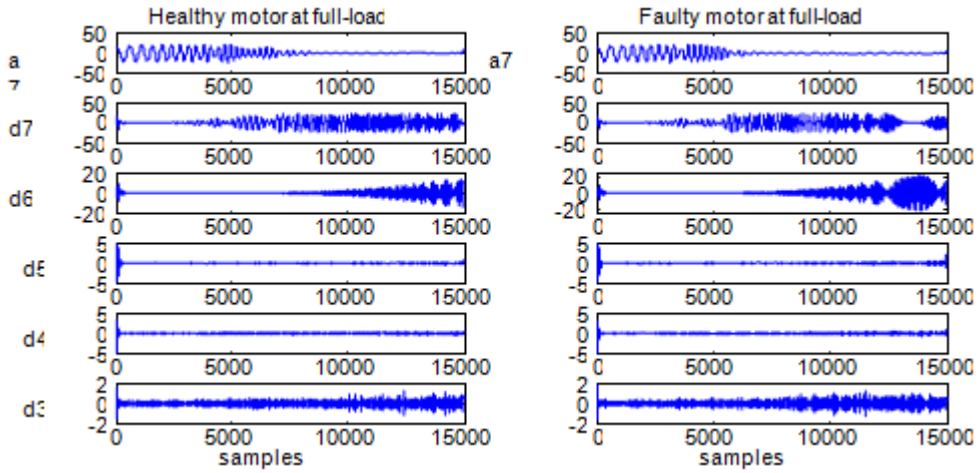

Figure 11: Wavelet Coefficient plot for motor at full-load

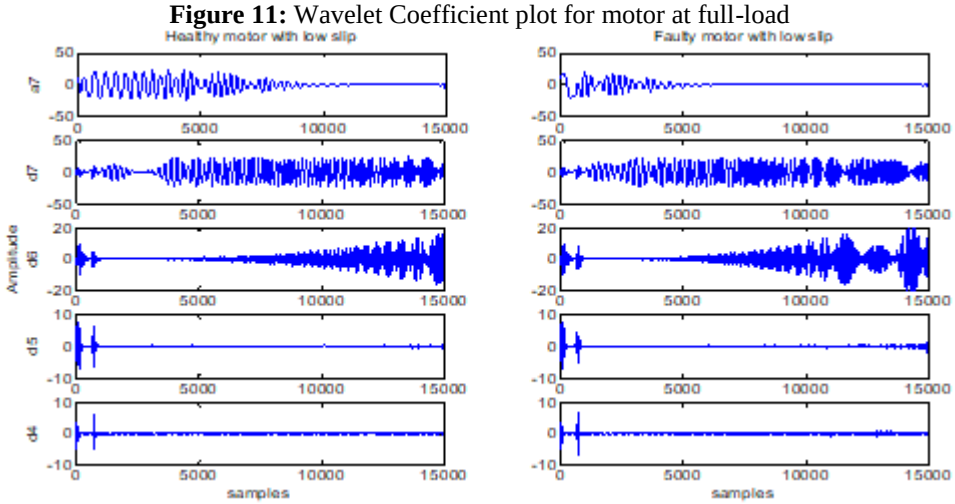

Figure 12: Wavelet coefficient plot of motor at full-load with reduced slip

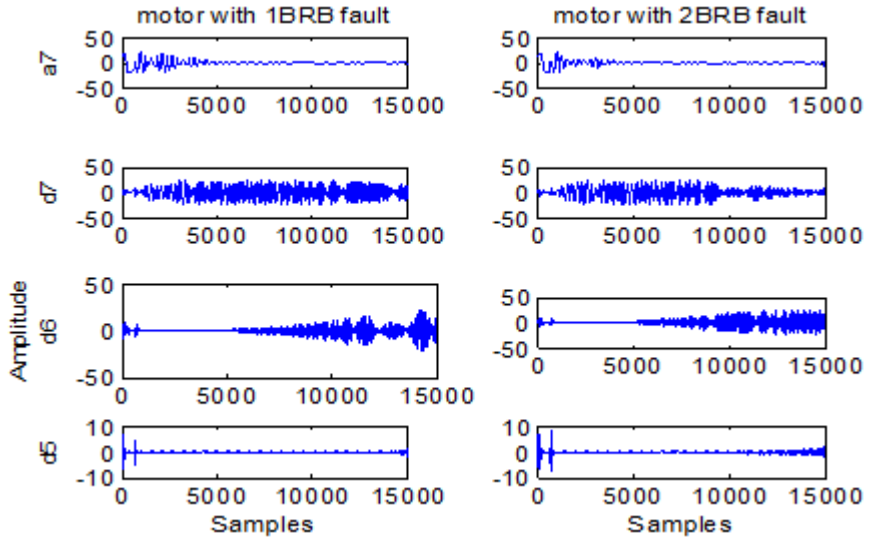

Figure 13: Wavelet coefficient plots for 1BRB and 2BRB fault motor at rated load

The result presented in fig.9 shows the coefficient plot for stator phase current at no-load, the plots of the coefficient of the seven levels of decomposition show no variation for both faulty motorand the healthy one. This is in-line with studies in literature where it has been difficult to identify BRB fault signatures using Fast Fourier Transform. Examining the coefficient plot for full-load (15N-m) operation presented in fig.10, the rotor speed is seen to rise faster in faulty condition than in healthy condition. Considering a closed-loop system with speed control loop, the motor tends to draw more current at faulty condition in order to produce speed that match desired torque output.

The coefficient plots presented in fig.11 show the detail three to detail seven as well as the approximate coefficient plot at level seven in order to have a wide frequency band for inspection. However, for decomposition levels from one to five (d1-d5), no information about signal variation was available. The low frequency detail-7 and detail-6 that corresponds to frequency bands of 19-39Hz and 39-78Hz respectively presented visible information that distinguished

healthy motor from faulty motor which proved relevant to this fault study.

Another simulation wascarried out with the same full-load parameters at low slip of 0.5% to investigate the performance of wavelet analysis. Similar results from the operation with slip of 0.9% was obtained as shown in fig.12.Though the effect of slip in BRB fault detection was visible, d7 and d6 remain valid for fault detection.

When the rotor bar resistance was increased further to test for severity such that two rotor bars are considered broken which gives incremental resistance value of 0.2225Ω, the plots shown in fig.13were obtained. Comparing the detail-7 and -6 coefficient plots for 1BRB and 2BRB faults, significant variations are seen on the plots, and detail 6 coefficient plot stands out in identifying fault presence.

4. Conclusion

Wavelet analysis has been successfully applied for detection of broken rotor bar fault in field oriented controlled induction motor. The detection algorithm decomposed the stator phase current using discrete wavelet transformation and plot coefficients of the detail levels that correspond to different frequency bands. The simulation results obtained show good results in BRB fault diagnosis, the high frequency components that lie within the frequency band above 78Hz show no variation, therefore are not relevant to fault detection. The low frequency details 6 and 7 that fall within 39 and 78Hz show significant variation at full-load condition because they covered the supply frequency (50Hz) and fault frequency.
By reducing the slip as well as increasing the severity of fault condition, detail 6 and 7 remains valid for fault detection. Sampling frequency is identified as a key factor responsible for having two levels consistent with fault presence, such precision of detection can be affected by sample frequency.

References

[1] Benbouzid. M. E. H., Theys. C. Vieira. M., "Induction Motors Faults Detection and Localization Using Stator Current Advanced Signal Processing Techniques,"*IEEE Trans. Power Electron*., vol.14, no.1, pp.14–22, Jan 1999.

[2] Thompson W.T, Rankin D. And Dorrell D.G, "On-Line Current Monitoring to Diagnose Air-Gap Eccentricity in Large Three-Phase Induction Motors, Industrial Case Histories Verify Predictions, *IEEE Transactions on Energy Conversion*, vol. 14, no. 4, pp.1372-1378, 2000.

[3] Acosta. G., Verucchi. C., and Gelso. E., "A Current Monitoring System forDiagnosing Electrical Failures in Induction Motors," *Mechanical Systems and Signal Processing*, vol. 20, no. 4, pp. 953–965, 2006.

[4] Henao. H., Capolino. G., Fernandez-Cabanas. M., Filippetti. F., Bruzzese. C., Strangas. E., Pusca. R., Estima. J., Riera. M., and Hedayati. S., "Trends in Fault Diagnosis for Electrical Machines: A Review of Diagnostic Techniques," *Industrial Electronics Magazine, IEEE*,vol. 8, No. 2, pp. 31–42, 2014.

[5] Cunha, M. C. C., and Cardoso, F. B. J., "Detection of Rotor Faults in Induction Motor Using Adjustable Speed Drives," Conference Record Of 2006 IEEE Industry Applications Conference Forty-First IAS Annual Meeting, Tampa, FL, pp.2354-2359, 2006

[6] Cristaldi, L., Faifer, M., Piegari, L., Rossi, M., and Toscani, S., "Rotor Fault Detection in Field Oriented Controlled Induction Machines" 2010 International Symposium of Power Electronics Electrical Drives Automation and Motion, pp. 529-534, 2010.

[7] Akin, B., U. Orguner, U., Toliyat, H. A., and Rayner, M., "Low Order PWM Inverter Harmonics Contributions to The Inverter-Fed Induction Machine Fault Diagnosis," IEEE Transactions on Industrial Electronics, vol. 55, no. 2, pp. 610-619, 2008.

[8] Bellini. A., Concari. C., Franceschini. G.,Tassoni. C., (2007) "Different Procedures for the Diagnosis of Rotor Fault in Closed Loop Induction Motors Drives", 2007 IEEE international Electric Machines & Drives Conference, Antalia, pp.1427-1433, May 2007.

[9] Cruz. S.M.A and Cardoso. A.J.M, "Strategies for The Diagnosis of Rotor Faults in Vector-Controlled Induction Motor Drives", 20th International Congress on Condition Monitoring and Diagnosis for Engineering Management, Faro, Portugal, pp.607-615, 2007.

[10] Szabo, L., Dobai, B., Biro, K.,Fodor, D., and Vass, J., "Wavelet Transform Approach to Faults Detection in Induction Motors", *8th IEEE International Conference on Intelligent Engineering Systems INES'2004*, Romania, pp. 397-402, May, 2004.

[11] Pons-Llinares, J., Antonino-Daviu, J., Roger-Folch, J., Morinigo-Sotelo, D., Duque-Perez, O., "Eccentricity Diagnosis in Inverter Fed Induction Motors via the Analytic Wavelet Transform of Transient Currents". *XIX International Conference on Electrical Machines (ICEM),* pp.1 -6, 2010.

[12] Antonino-Daviu. J., Rodriguez. P., Riera-Guasp. M., Pineda-Sandez M, Arkkio A., "Detection of Combined Faults in Induction Machines withParallel Branches Through theDWT of The Start-Up Current" , IEEE Transactions on Mechanical Systems and Signal Processing. 23, no. 7, pp. 2336-2351, 2009.

[13] Siddiqui, M. K., and Giri, V. K., "Broken Rotor Bar Fault Detection in Induction Motors Using Wavelet Transform", 2012 *International Conference on Computing, Electronic and Electrical Technologies, 2012.*

[14] Valens, C. "A Really Friendly Guide to Wavelets" Valens .C @mindless.com, 1999.

[15] Krishman K, "Electric Motor Drives; Modelling, Analysis and Control", Prentice hall, New-jersey, 2001.

[16] Chen. S., and Zivanovic. R., "Modelingand Simulation of Stator and Rotor Fault Conditions in Induction Machines for Testing Fault Diagnostic Techniques," *European Transactions on Electrical Power*, vol. 20, no. 5, pp. 611-629, 2009.